STIR

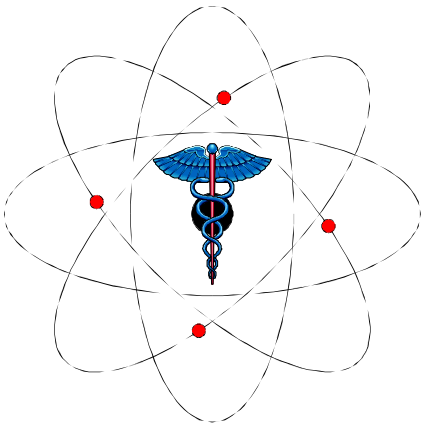

Description of the STIR implementation of FBP 3DRP

Authors: Claire Labbé, Habib Zaidi, Christian Morel. (Hôpital Cantonal de Genève)

(updated by Kris Thielemans, Hammersmith Imanet Ltd)

Version 0.91

1 INTRODUCTION

The reprojection algorithm of Kinahan and Rogers, so called 3DRP (3D Reprojection), or PROMIS (PROjection MISsing data) in the commercial implementation of CTI, is the most widely used 3D reconstruction algorithm. This algorithm is based on an exact method whereby the data incompleteness inherent in the 3D acquisition method is addressed by forward projection. The objective of this document is to explain the 3DRP reconstruction algorithm and give some details on the implementation in STIR.

This document is essentially a cut-down version of Deliverable 4.2 of the PARAPET project, with some minor modifications by Kris Thielemans. It lacks details on the actual implementation, a description of the parameters etc.

2 Description of 3DRP

2.1 Overview of the 3DRP Reconstruction Algorithm

Three-dimensional reconstruction is complicated by the fact that all the oblique 2D projections (corresponding in a multi-ring scanner to coincidences with a ring difference larger than one) are incompletely measured due to the finite length of the scanner (Figure II.1).

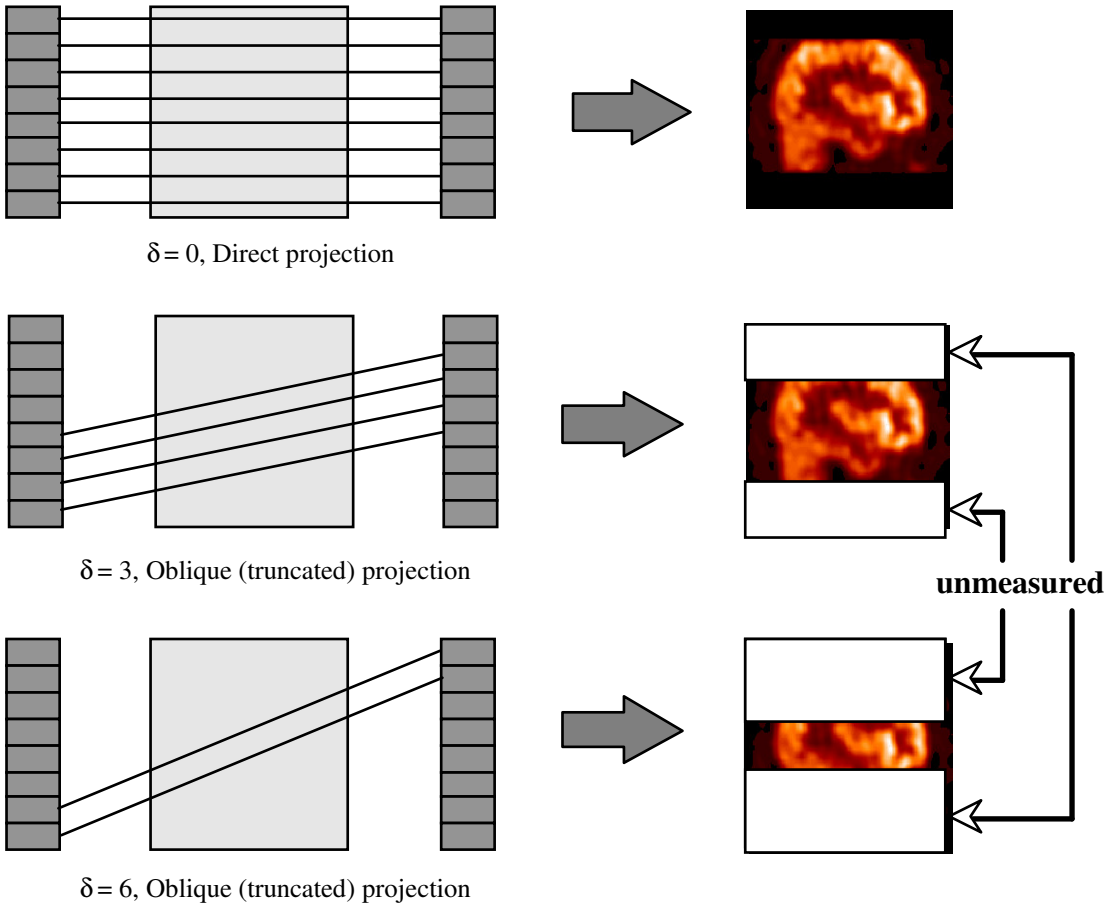

Figure II.1: *Projection truncation problem. Three different cases are illustrated here during the acquisition for oblique projections with a given ring difference δ.*

Kinahan and Rogers [Kinahan et al., 1989] proposed their reprojection method to work around the problem of axial shift variance or truncation of the projection data: a first estimate of the image is reconstructed using a sufficient data set satisfying Orlov's condition with all projections fully measured; this is usually the set of transaxial, or direct, projections. By calculating line integrals through this first image along the missing detection channels, the truncated parts of the projections (Figure II.2) can be recovered at all remaining angles. This is obtained by forward-projecting from a first image estimate what would have been detected by an axially longer scanner. Having artificially restored the axial shift invariance of the data, the image can be reconstructed by filtered backprojection (FBP) of the 2D projections using the Colsher filter.

Due to the hybrid nature of the data – oblique sinograms consist of data both measured and calculated by forward projection of a first image estimate – noise propagation properties and smoothing characteristics of this method become involved. The validity of this approach is however confirmed daily in practical use since the reprojection method is the most widely used 3D reconstruction algorithm and is implemented in most commercial 3D PET scanners.

The Colsher filtering and forward projecting algorithms are described later in this document. For general convention naming, please refer to the glossary of buildblocks in D4.1a.

2.2 More details on 3DRP

The main steps for 3DRP algorithm are as follows (Figure II.2):

• Reconstruction of an initial estimate of the image from direct and cross planes (*delta* or $\theta = 0$ and ±1) only using a 2D reconstruction technique (in this case, we use 2D FBP).

• Forward projection of this image estimate to complete the partially measured transaxial projections in oblique sinograms ($\theta \neq 0$ and ±1). If desired, $|\theta|$ can extend out to θ_{max}, the maximum acceptance angle of the tomograph (Fig. II.3). However, at these angles, the number of measured LORs may be small compared with the number that has been obtained by reprojection (Fig. II.2).

• With a set of complete projections for all $|\theta| \leq \theta_{max}$, reconstruct a final image incorporating all sinograms by FBP using the Colsher filter. In an ideal situation of continuously sampled and noise-free data, the final image obtained from the third step would be identical to the initial estimate from the first step. Actually, due to the statistical nature of the data which results from a counting experiment, the incorporation of the additionnal oblique LORs improves significantly the signal to noise of the final 3D reconstruction by a factor of about 6.

In the 3DRP reconstruction algorithm, according to the above section, there are three specific building blocks:

- Colsher's filtering,
- Forward projection,
- Reconstruction kernel.

In summary, the 3DRP algorithm executes the following steps as shown in Figure II.2:

• 2D FBP (reconstruct the direct projections (2D FBP) in order to have an first 2D estimate of the image)
- Extract 1D transaxial projections,
- Filter 1D transaxial projections (using a Ramp filter, apodized or not),
- 2D backproject the filtered projections.

• 3D FBP

- Extract 2D projections,
- Filter 2D using Colsher's filter + 2D backproject,
- Forward project missing data calculated from the 2D estimate of the image,
- Filter 2D using Colsher's filter,
- 3D backproject completed projections.

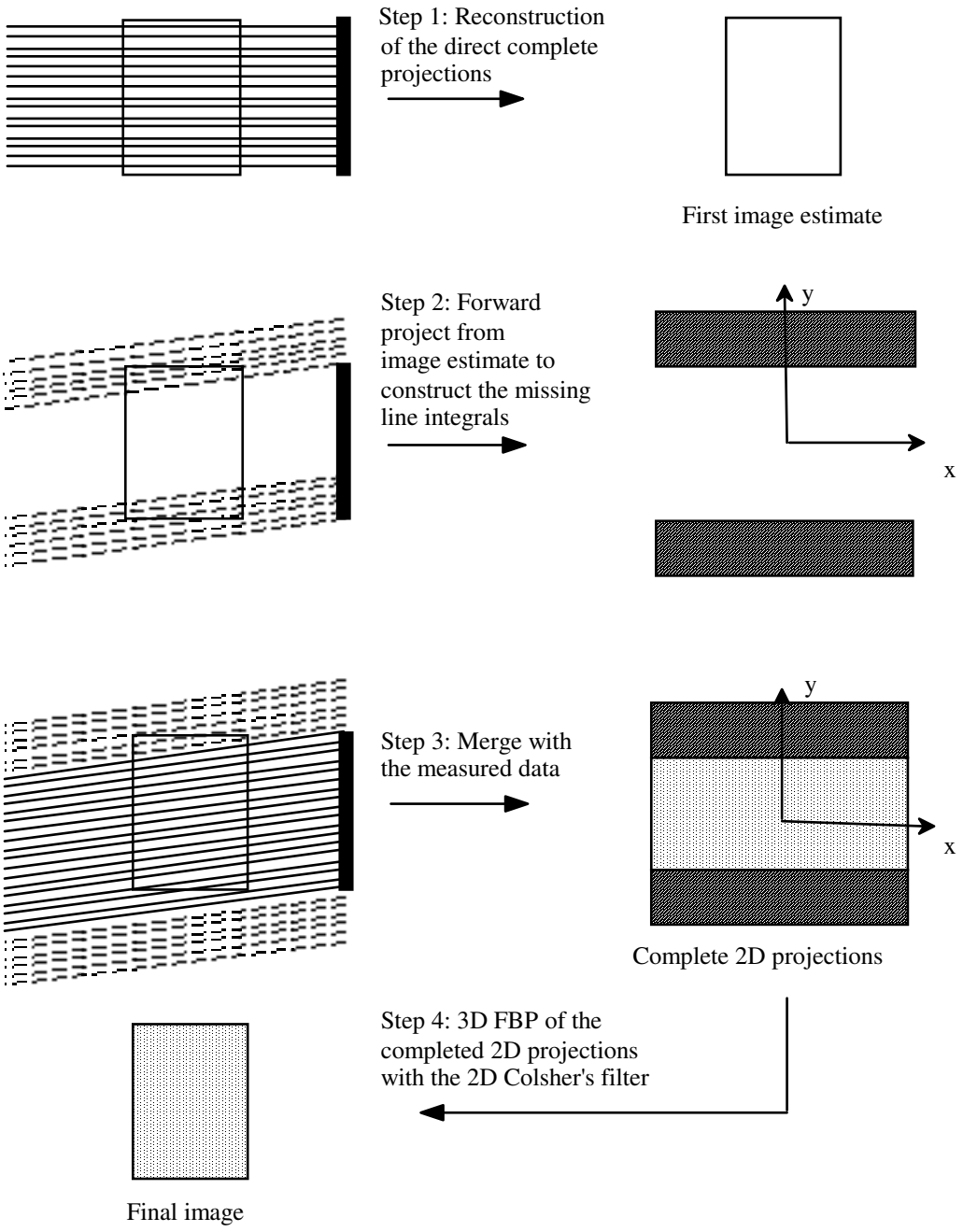

Figure II.2: Reprojection algorithm sometimes dubbed the "3DRP" algorithm.

2.3 Colsher Filter

2.3.1 Algorithm

This filter was originally derived by Colsher (1980) for the case of a shift-invariant scanner with limited acceptance θ_{min} (Fig. II.3). His initial derivation was based on a relation between the activity distribution $f(\vec{x})$ and the backprojected image of the unfiltered projections, in a backproject-then-filter framework.

In a scanner with a spatially invariant point spread function *h* resulting from the backprojected projections of a single object point, these quantities are linked by the relation

$$g(\vec{x}) = \int f(\vec{x}')h(\vec{x} - \vec{x}')d^3\vec{x}' . \qquad \text{(Eq. 1)}$$

Recovery of the activity distribution $f(\vec{x})$ then requires the inversion of Equation 1, which may be written in Fourier space as the deconvolution process

$$F(\vec{\nu}) = G(\vec{\nu})Q^{-1}(\vec{\nu}) = G(\vec{\nu})H_{Colsher}(\vec{\nu}), \qquad \text{(Eq. 2)}$$

with $H_{Colsher}(\vec{\nu}) = Q^{-1}(\vec{\nu})$ is the Colsher filter. More detailed developments may be found in [Colsher, 1980]. The Colsher filter can be expressed by the following transfer function:

$$H_{Colsher}(\vec{\nu}) = \begin{cases} \dfrac{|\vec{\nu}|}{2\pi} & \text{if } \cos\psi \geq \cos\theta_{\max} \quad (\textit{Figure II.4.A}) \\ \dfrac{|\vec{\nu}|}{2\pi} \dfrac{1}{\arcsin(\sin(\theta_{\max} / \sin\psi)} & \text{if } \cos\psi < \cos\theta_{\max} \quad (\textit{Figure II-4.B}) \end{cases} \qquad \text{(Eq. 3)}$$

where ψ is the polar angle of the frequency vector(i.e $\nu_z/|\vec{\nu}| = \cos\psi$), $\theta_{\max}$ the maximum aperture angle included in the reconstruction theta_max = $\theta_{\max}$ = atan(r_S*(maxdelta)/(2*R). The maximum ring difference *maxdelta* cannot exceed the number of detectors rings minus two. r_S, is the ring spacing and R the ring radius.

Note thate there is no azimuthal angular dependence for the filter , which is a consequence of the rotational symmetry of the PET scanner around the *z*-axis. So the Colsher filter depends only on $\vec{\nu}$, and not on (ϕ, θ).

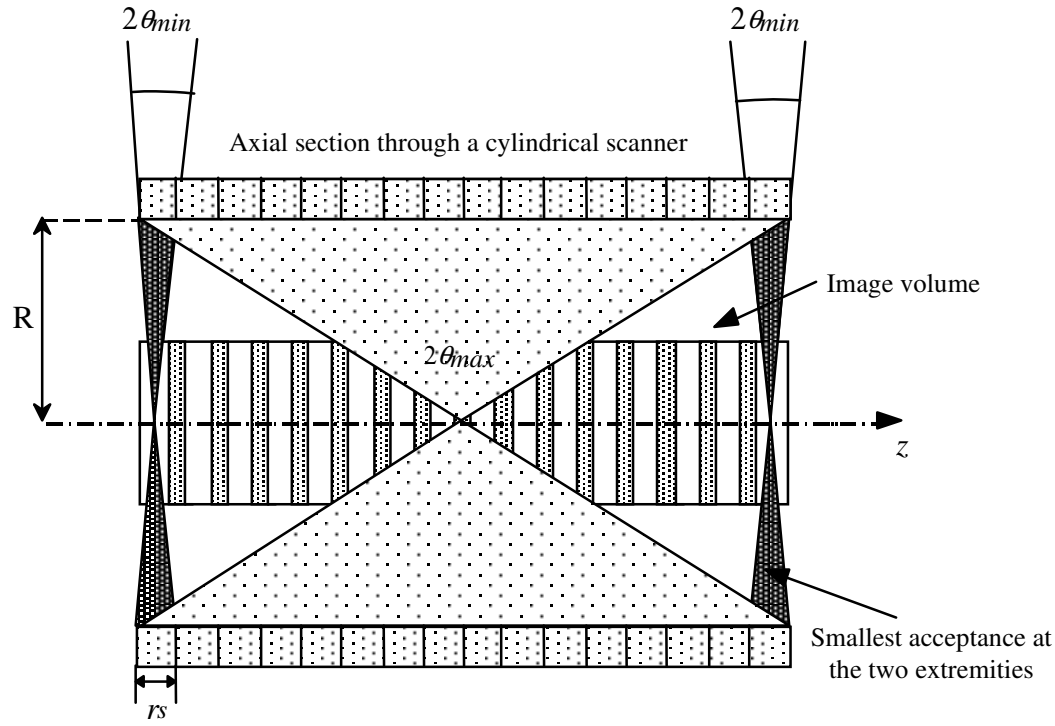

Figure II.3: *The acceptance angle θ of a cylindrical scanner varies within the field of view. The largest acceptance, θ_{max}, is found at the centre, whereas the minimum value θ_{min} corresponds to the aperture of the first and last image slices, at the extremities of the scanner.*

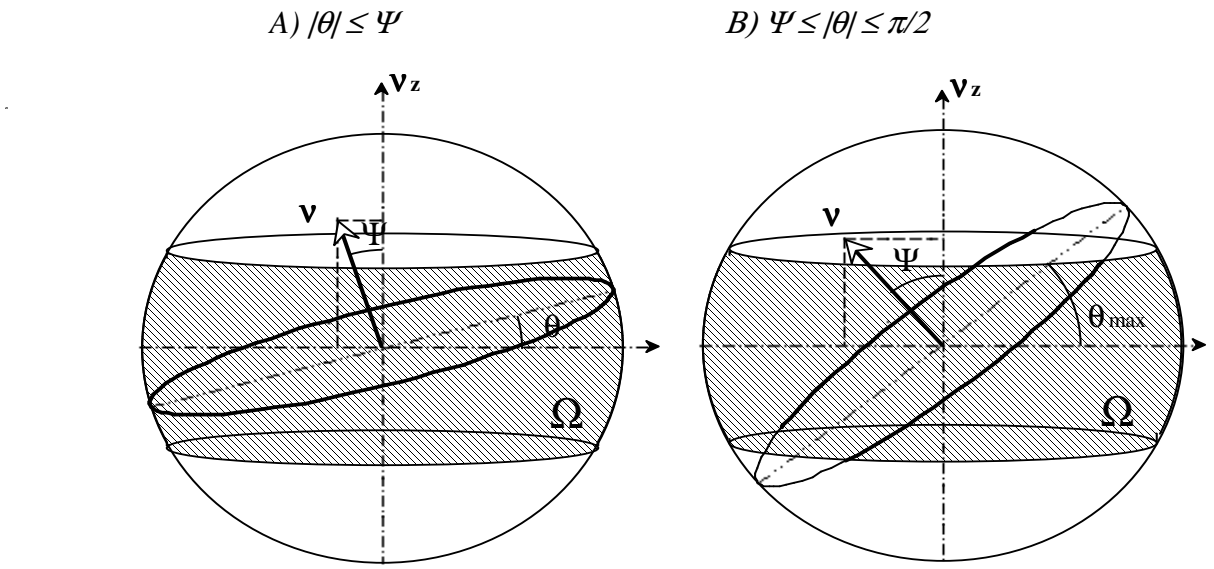

Figure II.4: *In the Colsher filter, for any frequency vector $\vec{\nu}$, the 2D Ramp filter has to be weighted by the arc length of the intersection between the great circle perpendicular to $\vec{\nu}$ with the set of measured directions of projection Ω*

represented on the unit sphere. Thus, the Colsher filter can be split into 2 regions depending on whether the great circle perpendicular to $\vec{v}$ is contained in Ω or not.

A generalized Hamming apodizing window $\alpha+(1-\alpha)\cos(\pi v/ v_a)$ has been included in the Colsher filter in order to limit the amplification of statistical noise. The parameter α in the apodizing function allows to control the noise amplification due to the Ramp filter. The Colsher filter is one of an infinite number of possible filters allowing exact 3D reconstruction, but due to its minimum norm property, it has the minimum noise amplification properties [Defrise, 1989].

2.3.2 Implementation of the Colsher filter

The filtering step is performed using the STIR FFT routines, which require the array dimensions to be integer powers of two. Aliasing in the discrete convolution is avoided by padding the data to a power of two greater (or equal) to twice the data size. [1]

Similarly to in the 2D case, there is a problem with the DC (and very low frequency) components of the filtered data if the Colsher filter is simply sampled in frequency space. It is well-known that sampling should occur in the spatial domain instead. In the STIR implementation of 2D FBP this is done by computing an analytic inverse fourier of the ramp filter and sampling that spatial function. However, the Colsher fiter cannot analytically be transformed. Instead, we approximate this procedure by

- sampling the Colsher filter in frequency space at a high sampling rate
- numerically inverse DFT to the spatial domain
- sub-sample Colsher filter in spatial domain to the desired sampling size (given by the sampling of the projection data)
- numerically DFT to the frequency domain

As the Colsher filter is independent of the azimuthal angle, this procedure has to be done only a few times per reconstruction. The amount of sub-sampling is determined by the 'Stretch factor for Colsher filter definition in planar direction' parameter (and similar for axial direction).

2.4 Forward Projection

2.4.1 Description

The forward projection function allows to estimate the unmeasured data for oblique sinograms with $|\theta| > \pm 1$. The problem of how to complete the partially-measured projections of the truncated projections is detailed here.

2.4.2 Extending the effective axial length of the scanner (rmin and rmax)

The 3DRP algorithm necessitates the estimation of a number of unmeasured sinograms so as to satisfy the condition of axial shift invariance. These synthetic sinograms are found by forward-projecting an estimate of the image reconstructed from direct projections. Ray-tracing methods are particularly appropriate for the forward projection step.

[1] If desired, this can be reduced by a factor by setting the 'Transaxial extension for FFT' parameter to 0. However, this should only be done if the data indeed zero for half the FOV. As there are likely tails from remaining scatter or randoms, this is ***not recommended***.

The forward projection processing which was carried out with the implementation of Siddon's algorithm [Siddon et al., 1985], allows to estimate unmeasured oblique projection data which depend mainly on the number of elements in the unmeasured parts of the oblique projections. The forward projecting step estimates all the truncated projection data on fictive rings and is equivalent to simulate a PET scanner with a longer axial length.

The problem of how to complete the partially-measured projections can be resolved by using one set of complete projections that are measured (i.e direct projections with $\theta = 0$) to reconstruct an initial image using 2D FBP. With ths initial image, it is then possible to simulate the projection process mathematically and to create the unmeasured parts of a projection by "forward projecting" along LORs that do not exist in the actual tomograph as shown in Figure II.5. In practice, the unmeasured samples are grouped together into "missing sinograms corresponding to ring indexes outside the physical range of the tomograph.

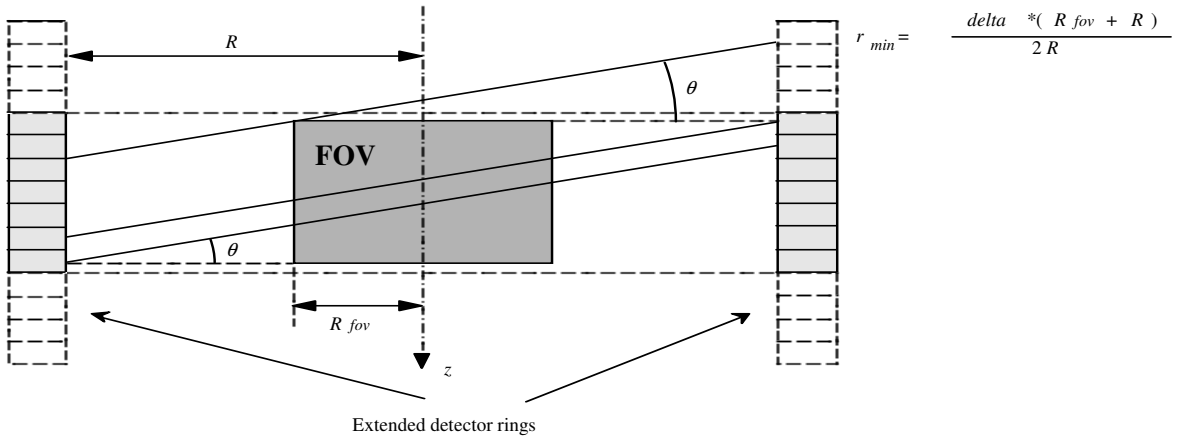

Figure II.5: *Extending the effective axial length of the scanner by forward projection (here $\psi < \Psi$)*

The calculation of the lower and upper bound ring numbers of the extra detectors rings *rmin* and *rmax* is based on the following formula:

$$\tan(theta) = \frac{r_{\min} \times r_s}{R_{fov} + R} = \frac{delta \times r_s}{2R} \quad => \quad r_{\min} = \frac{delta * (R_{fov} + R)}{2R} \qquad \text{(Eq. 5)}$$

where R_{fov} is the FOV radius,*R* the ring radius, and *delta* the ring difference of the corresponding oblique sinograms.

The rmax value is calculated as follows :

$$rmax = num\_rings - min - 1 - delta \qquad \text{(Eq. 6)}$$

In the actual code, there is an adjustment of this formula for the case of axial compression (*span*) as the sampling in z position is different in that case.

Note that the maximum ring difference which is used for the 3D reconstruction can be arbitrarily chosen up to the maximum aperture of the tomograph defined by $\theta_{\max}$. The number of additional rings depends obviously on the axial and transaxial dimensions of the FOV that is to be reconstructed. In fact, the amount of forward projected data increases rapidly for larger ring differences, such that the amount of the measured data incorporated is only increasing slowly.

Typically, the maximum ring difference which used for the 3D reconstruction is chosen so that the number of forward projected sinograms is about the same than the number of measured sinograms.

3 REFERENCES

Cherry S.R, Dahlbom M, and Hoffman E.J (1992) "Evaluation of a 3D reconstruction algorithm for multi-slice PET scanners,", Physics in Medicine and Biology, 37(3), p. 779-790, p. 103-115.

Colsher J G (1980) "Fully three-dimensional positron emission tomography," Physics in Medicine and Biology, 25(1), p. 103-115.

Defrise M., Townsend D.W. and Clack R. (1989) "Three-dimensional image reconstruction from complete projections,". Phys Med Biol. 34:5:573-587.

Egger M L (1996) "Fast Volume Reconstruction in Positron Emission Tomography: Implementation of Four Algorithms on a High-Performance Scalable Parallel Platform," PhD Thesis, University of Lausanne.

Kinahan P E and Rogers J G (1989), "Analytic 3D image reconstruction using all detected events," IEEE Transactions on Nuclear Science, 36-1, p. 964-968.

Siddon R L (1985) "Fast calculation of the exact radiological path for a three-dimensional CT array," Medical Physics, 12-2, p. 252-255.